Accuracy and Cost Computation of the EM Coupling of a Cellular Handset and a Human Due to Artifact Rotation

Salah I. Al-Mously, *Student Member, IEEE,* Abdulgader Z. Abdalla, Marai M. Abousetta and E. M. Ibrahim

Abstract — **This paper investigates both the computation accuracy (based on the power balance error) and the cost in terms of the number of FDTD-grid cells due to the artifact rotation for a cellular handset close to the user's head. Two study cases are simulated to assess the EM coupling of a cellular handset and a MRI-based human head model at 900 MHz; firstly, both handset and head CAD models are aligned to the FDTD-grid, secondly, handset close to a rotated head in compliance with IEEE-1528 standard. A FDTD-based platform, *SEMCAD-X*, is used; where conventional and interactive gridder approaches are implemented to achieve the simulations. The results show that owing to the artifact rotation, the computation error may increase up to 30%, whereas, the required number of grid cells may increase up to 25%.**

Keywords — **Computational dosimetry, FDTD, Handset, MRI-based phantoms.**

I. Introduction

THE problem of calculating energy absorption in human head when exposed to the electromagnetic radiation of cellular handsets has been under consideration for the past two decades. This energy is measured by predicting the induced specific absorption rate (SAR) in the user's head-tissues [1]-[22].

The protocol and procedures for the measurement of the peak spatial-average SAR induced inside a simplified head model of the cellular handset users are specified by IEEE Standard-1528 [23] and IEC 62209-1 [24]. An algorithm based on SCC34/SC2/WG2 computational dosimetry, IEEE Standard-1529 [25], the spatial peak SAR(x, y, z, f_o) can be computed over any required mass.

The human head model and the RF source are the two half's of any computational RF dosimetry, and the implications in computing the EM coupling of different handset models and different head models in the previous works are well addressed and reviewed in [26].

Analytical techniques using Finite-Difference Time-Domain (FDTD) [1]-[22] or FDTD with the Method of Moment (MoM) [4] or FDTD with semi-analytical method (Green/MoM) [9] were employed to study the EM coupling between human head and cellular handset antennas.

Dipole antenna [9], [10], [22], metal box with either internal or external antenna [1]-[17], semi-realistic CAD-models with real configuration [18]-[20] and very realistic CAD-models [21], [27] were used to simulate the cellular handset in computing its EM coupling with the human head. Homogeneous sphere [1], [4], homogeneous Specific Anthropomorphic Mannequin (SAM) [17], [19]-[21], [27] and heterogeneous Magnetic Resonance Identification (MRI)-based [5]-[22] CAD-models were used to simulate the human head.

In [5]-[22] where MRI-based anatomically correct models were used to simulate the human head, scarcely in [5]-[10], [22] both handset and human head tissues are aligned to FDTD-grid, whereas, in [11]-[21] the handset is aligned to FDTD-grid but the head is rotated, simulating practical usage of the cellular handset.

In this work a FDTD-based platform *SEMCAD-X* [28] is used to compute the EM coupling and investigate both the computation accuracy and the cost in term of number of FDTD-grid cells due to the user's head rotation in compliance with the IEEE Standard-1528 [23].

II. FDTD Modeling

The FDTD method proposed by Yee in 1966 [29] is a direct solution of Maxwell's curl equations in the time domain. Maxwell's curl equations are discretized using a 2^{nd} order finite-difference approximation both in space and in time in an equidistantly spaced mesh [28].

The *SEMCAD-X* simulation platform is selected for simulating the study cases in this work due to its handling, functionality and features for highly detailed CAD models as well as efficient FDTD solver for simulating advanced applications. *SEMCAD-X* is a 3-D

S. I. Al-Mously is with the Department of Microwave and Radar Engineering, The Higher Institute of Electronics, P.O. Box (38645), Beni-Walid, Libya. Currently he is working toward the Ph.D. degree at the School of Applied Sciences and Engineering, Academy of Graduate Studies, P.O. Box (79031), Janzoor, Triploi, Libya (phone: +218-913-675265; Fax: +218-315-242334; e-mail: salah.mously@ieee.org).

A. Z. Abdalla is with the Department of Microwave and Radar Engineering, The Higher Institute of Electronics, P.O. Box (38645), Beni-Walid, Libya; (e-mail: azazgbwl@yahoo.com).

M. M. Abousetta is with the Department of Microwave and Radar Engineering, The Higher Institute of Electronics, P.O. Box (38645), Beni-Walid, Libya; (e-mail: maraibusetta@yahoo.co.uk).

E. M. Ibrahim is with the Department of Microwave and Radar Engineering, The Higher Institute of Electronics, P.O. Box (38645), Beni-Walid, Libya; (e-mail: embarakibrahim@yahoo.co.uk).

full wave simulation environment based on the FDTD method.

A semi-realistic handset CAD model with a short-whip antenna top loaded with a small cylinder [20] is simulated with its real configuration and designed to operate at frequency of 900 MHz. The considered handset electromechanical parts are; *antenna, antenna cover, PCB, shields, LCD and its holder, housing parts, keypad and buttons, battery and battery contacts, and connectors*. The dielectric parameters of the handset materials given in [21] are used. The maximum dimensions of the proposed handset model are set to 43 × 16.5 × 104 mm^3. Referred to the IEEE Standard-C95.1b-2004 [30] (for low power devices, uncontrolled environment) the antenna input power is set to 0.6 W. Fig. 1 shows the handset CAD model with antenna structure and dimensions.

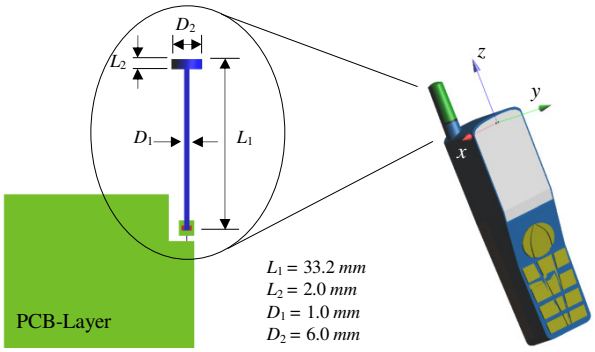

Fig. 1. A 3-D view of the handset CAD model with antenna structure and dimensions.

A heterogeneous MRI-based head model, High Resolution of a European Female Head (HR-EFH) [31], available with SPEAG – Schmidt & Partner Engineering AG [28] is used. This phantom consists of 121 different slices, with slice thicknesses of 1 mm (ear region) and 3 mm and a transverse spatial resolution of 0.2 mm. The following different twenty five tissues are recognized: *Air, Blood vessel, Boons, Brain/grey matter, Brain/white matter, Cerebellum, Cerebrospinal Fluid, Ear (cartilage), Eye-cornea, Eye-lens, Eye-vitreous body, Fat, Jaw, Mastoid cells (bones), Mid-brain, Muscles, Nasal cavity, Parotid Gland, Spin, Skull, Spinal cord, Spine, Thalamus, Tongue and Ventricles*. Tissues properties are set according to material properties data-base in [28], [32].

III. Rotation Artifacts and FDTD Grid Consideration

In many published works, authors were intended to align both handset and MRI-based human head to the FDTD-grid, where the handset and the head are vertically parallel to each other in order to avoid the stair-step effect [5]-[10], [22]. This is not the practical usage of the cellular handset as in compliance with the IEEE Standard-1528 [23] the rotation of head with respect to handset is compulsory. The problems that should be considered in modeling a rotated user's head and the artifacts of the voxelized models after re-meshing are well explained in [26].

To evaluate the computation accuracy of the EM coupling of a handset close to a rotated and non-rotated MRI-base head model and to investigation the capability of the *SEMCAD*-platform in decreasing the effects owing to the rotated head model, two study cases are proposed:

1. A handset closed to a MRI-based head model and both are aligned to the FDTD-grid, as shown in Fig. 2-(a).
2. A handset closed to a MRI-based head model at *cheek* position, where the handset is aligned to FDTD-grid, whereas, the human head is rotated by (60^o) according to IEEE standard 1528 [23], as shown in Fig. 2-(b). Fig. 3 shows the voxelized model after re-meshing.

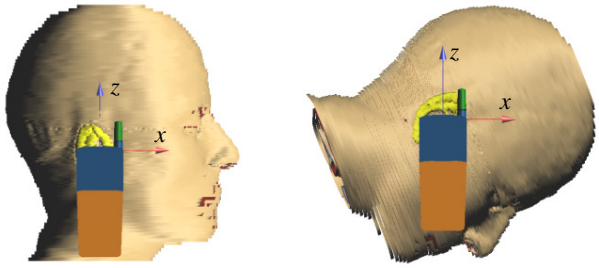

(a) (b)

Fig. 2. CAD representations of the handset close to the; (a) non-rotated HR-EFH phantom and (b) rotated HR-EFH phantom.

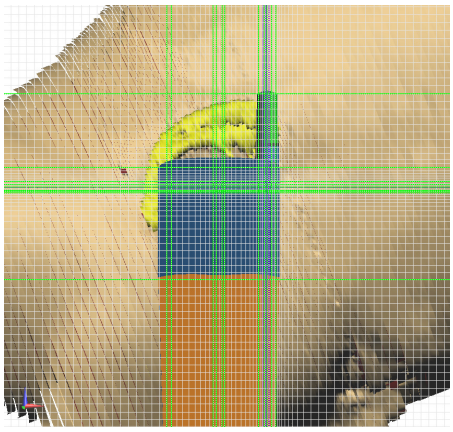

Fig. 3. Mesh cells of the voxelized handset close to head model. The handset is aligned to FDTD-grid, while the head is rotated by (60^o).

As in [33], we adopted the computed power balance relative error to be the measure of the computation error;

$$\text{Computation error} = |P_{in} - (P_{rad} + P_{abs} + P_{Loss})| \,/\, P_{in} \quad (1)$$

$$P_{loss} = P_d + P_c \quad (2)$$

Where P_{in} is the input power, P_{rad} is the radiated power, P_{abs} is the absorbed power in tissues and P_{loss} is the total

power loss. P_{loss} includes both the dielectric-loss (P_d) and the metallic ohmic-loss (P_c) in the handset. Since all metal parts are considered as PEC in simulations, thus, $P_c = 0$.

In this work both (*SEMCAD-X*, ver. 12.0 JUNGFRAU) and (*SEMCAD-X*, ver. 12.4 JUNGFAU) platforms are used to achieve conventional and interactive gridding, respectively. The conventional gridder setting has a minimum spatial resolution of 0.5 × 0.5 × 0.5 mm^3 and a maximum spatial resolution of 8 × 8 × 8 mm^3 in the *x*, *y*, and *z* directions with grading ratio of 1.2. The interactive gridder setting has a baseline resolution of 0.001 λ and a maximum step of 0.05 λ with a grading ratio of 1.2 and grading ratio relaxation of 10%. A local setting for the antenna is made with a local scale factor of 0.8 and both baseline resolution and maximum step of 0.001 λ. For both conventional and interactive gridder setting a refining factor of 10 is set for all solid regions. During the simulation processes, the absorbing boundary conditions (ABC) are set as a Uniaxial Perfectly Matched Layer (UPML) mode with a very high strength thickness, where a minimum level of absorption at the outer boundary is >99.9% [28].

IV. Results and Inferences

Table 1 shows the antenna specifications of the handset in free space and the handset close to the non-rotated and rotated head at *cheek* position. These specifications are calculated for both conventional and interactive gridder approaches including; the input impedance, $|S_{11}|$ in dB, radiation efficiency and total efficiency. To achieve better input return loss, the antenna is matched with a 15.25 nH lumped element.

TABLE 1: ANTENNA PARAMETERS OF THE HANDSET IN BOTH CASES FOR THE CONVENTIONAL AND INTERACTIVE GRIDDER APPROACHES.

Parameter	*Antenna Input Impedance (Ω)*	*$\|S_{11}\|$ (dB)*	*Radiation Efficiency*	*Total Efficiency*
Handset in free-space	43.3 + j 1.80	-22.48	76.13%	75.70%
Conventional approach				
Case (1)	45.6 + j 15.3	-15.66	26.13%	25.43%
Case (2)	35.1 + j 15.3	-12.13	17.80%	16.70%
Interactive approach				
Case (1)	48.7 + j 13.4	-17.37	26.18%	25.70%
Case (2)	37.0 + j 12.9	-13.62	17.90%	17.12%

Table 2 and Table 3 depict the averaged peak SAR over 1g in head tissues, radiated power, power absorption in head, dielectric loss and the percentage computation error for the handset closed to the non-rotated and rotated head model utilizing both conventional and interactive gridder approaches, respectively.

According to the results listed in Tables 1, 2 and 3, the antenna parameters, SAR and power losses are almost the same for both conventional and interactive approaches, but the following are noticed:

1. For the conventional gridder approach, the number of grid cells needed in case 1 is about 80% of that needed in case 2. In case 1 the computation error is 2.85%, whereas, it is 3.7% in case 2.
2. For the interactive gridder approach, the number of grid cells needed in case 1 is about 48.7% of the number needed in case 2. In case 1 the computation error is 1.79%, whereas, it is 1.99% in case 2.

It is obvious that the artifact rotation of human head to realize the actual usage of a cellular handset implies more number of grid cells and produces higher computation error. The interactive gridder approach has lesser computation error increase due to the artifact rotation, 11.1%, as compared with the conventional approach which has a computation error increase of 30%.

TABLE 2: TOTAL NUMBER OF GRID-CELLS, SAR_{1g} AND POWER LOSS IN TISSUES, AND THE COMPUTATION ERRORS FOR THE CONVENTIONAL GRIDDER APPROACH.

Head position	*Aligned*	*Rotated*
Number of FDTD-Grid Cells (Mcells)	15.583	19.4637
Input power (mW)	600	600
Peak-SAR_{1g} (W/kg) in head	3.45	4.79
Radiated power (mW)	152.57	100.23
Absorbed power in head (mW)	309.08	329.25
Absorption rate in head (%)	51.51	54.88
Dielectric-loss (mW)	121.25	148.32
Computation error (%)	2.85	3.70

TABLE 3: TOTAL NUMBER OF GRID-CELLS, SAR_{1g} AND POWER LOSS IN TISSUES, AND THE COMPUTATION ERRORS FOR THE INTERACTIVE GRIDDER APPROACH.

Head position	*Aligned*	*Rotated*
Number of FDTD-Grid Cells Mcells)	9.27769	19.0608
Input power (mW)	600	600
Peak-SAR_{1g} (W/kg) in head	3.43	4.81
Radiated power (mW)	154.23	102.75
Absorbed power in head (mW)	310.40	333.76
Absorption rate in head (%)	51.73	55.63
Dielectric-loss (mW)	124.63	151.56
Computation error (%)	1.79	1.99

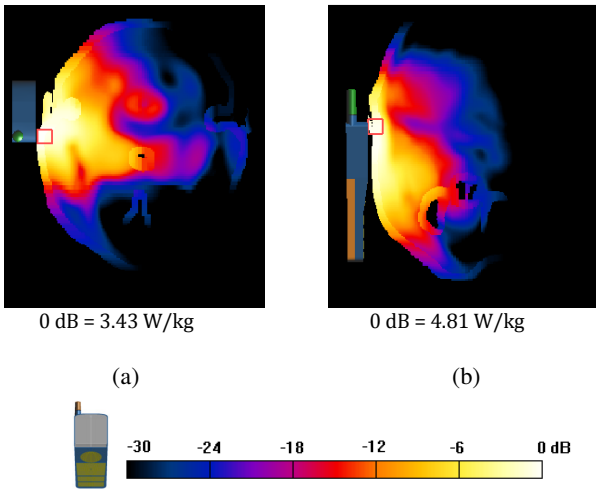

Fig. 4. Sliced-distribution of the averaged peak SAR_{1g} induced in the HR-EFH phantom due to the handset exposure in the; (a) *xy*-plane, case 1, and (b) *yz*-plane, case 2.

Fig. 4 shows the sliced-distribution of the averaged peak SAR_{1g} induced in the HR-EFH phantom exposed to EM radiation of the handset in both case1 and case 2.

All computations were performed on a 2 GHz Intel centrino™ Laptop machine (Dell, inspiron-630m) with 2 GB memory. The maximum number of grid-cells the machine can process is 21 Mcells, where no hardware accelerator aXware is used [28]. The runtime and memory requirements depend on the simulation space as well as the refinement factor for each solid region, where the maximum runtime was about 8 hrs.

REFERENCES

[1] J. Toftgard, S. N. Hornsleth, and J. B. Andersen, "Effects on portable antennas of the presence of a person," *IEEE Transaction on Antennas and Propagation*, vol. 41, no. 6, pp. 739-746, 1993.

[2] M. A. Jensen and Y. Rahmat-Samii, "EM interaction of handset antennas and a human in personal communications," *IEEE Proceeding*, vol. 83, no. l, pp. 7-17, 1995.

[3] J. Graffin, N. Rots and G. F. Pedersen, "Radiations phantom for handheld phones," in *Proc. Vehicular Technology Conference, IEEE VTS-Fall VTC-2000 52nd*, Volume 2, 2000, pp. 853 – 866.

[4] N. K. Kouveliotis, S. C. Panagiotou, P. K. Varlamos and C. N. Capsalis, "Theoretical approach of the interaction between a human head model and a mobile handset helical antenna using numerical methods," *Progress In Electromagnetics Research*, PIER 65, pp. 309–327, 2006,

[5] S. Khalatbari, D. Sardari, A. A. Mirzaee, and H. A. Sadafi, "Calculating SAR in Two Models of the Human Head Exposed to Mobile Phones Radiations at 900 and 1800MHz," in *Proc. Progress In Electromagnetics Research Symposium*, Cambridge, USA, March 26-29, 2006, pp. 104-109.

[6] M. Okoniewski and M. Stuchly, "A study of the handset antenna and human body interaction," *IEEE Transaction on Microwave Theory and Techniques*, vol. 44, no. 10, pp. 1855-1864, 1996.

[7] P. Bernardi, M. Cavagnaro and S. Pisa, "Evaluation of the SAR distribution in the human head for cellular phones used in a partially closed environment," *IEEE Transactions of Electromagnetic Compatibility*, vol. 38, no. 3, pp. 357-366, 1996.

[8] G. Lazzi, S. S. Pattnaik, C. M. Furse, and O. P. Gandhi, "Comparison of FDTD computed and measured radiation patterns of commercial mobile telephones in presence of the human head" *IEEE Transaction on Antennas and Propagation*, vol. 46, no. 6, pp. 943-944, 1998.

[9] Stavros Koulouridis and Konstantina S. Nikita, "Study of the coupling between human head and cellular phone helical antennas," *IEEE Transactions of Electromagnetic Compatibility*, vol. 46, no. 1, pp. 62-70, 2004.

[10] J. Wang and O. Fujiwara, "Comparison and evaluation of electromagnetic absorption characteristics in realistic human head models of adult and children for 900-MHz mobile telephones," *IEEE Transactions on Microwave Theory and Techniques*, vol. 51, no. 3, pp. 966-971, 2003.

[11] G. Lazzi and O. P. Gandhi, "Realistically tilted and truncated anatomically based models of the human head for dosimetry of mobile telephones" *IEEE Transactions of Electromagnetic Compatibility*, vol. 39, no. 1, pp. 55-61, 1997.

[12] J. T. Rowley and R. B. Waterhouse, "Performance of shorted microstrip patch antennas for mobile communications handsets at 1800 MHz", *IEEE Transaction on Antennas and Propagation*, vol. 47, no. 5, pp. 815-822, 1999.

[13] S. Watanabe, M. Taki, T. Nojima, and O. Fujiwara, "Characteristics of the SAR distributions in a head exposed to electromagnetic field radiated by a hand-held portable radio," *IEEE Transaction on Microwave Theory and Techniques*, vol. 44, no. 10, pp. 1874-1883, 1996.

[14] P. Bernardi, M. Cavagnaro, S. Pisa and E. Piuzzi, "Specific absorption rate and temperature increases in the head of a cellular-phone user," *IEEE Transaction on Microwave Theory and Techniques*, vol. 48, no. 7, pp. 1118-1126, 2000.

[15] S. I. Al-Mously and M. M. Abousetta, "Study of Both Antenna and PCB Positions Effect on the Coupling Between the Cellular Hand-Set and Human Head at GSM-900 Standard," presented at the iWAT IEEE-2008, International Workshop on Antenna Technology 2008, "Small Antennas and Novel Metamaterials", Chiba, Japan, pp. 513-517, March 4-6, 2008.

[16] Lee, H. Choi, H. Lee H and J. Pack, "Human head size and SAR characteristics for handset exposure," *ETRI Journal*, vol. 24, pp.176-179, 2002.

[17] B. Beard, W. Kainz, T. Onishi, *et al*., "Comparisons of computed mobile phone induced SAR in the SAM phantom to that in anatomically correct models of the human head," *IEEE Transactions of Electromagnetic Compatibility*, vol. 48, no. 2, pp. 397–407, 2006.

[18] S. Francavilla, P. Bertotto and G. Richiardi, "Effect of the hand on cellular phone radiation," *IEE Proc. Microwaves, Antennas and Propagation*, vol. 148, pp. 247-253, 2001.

[19] Salah I. Al-Mously and Marai M. Abousetta, "A novel cellular handset design for an enhanced antenna performance and a reduced SAR in the human head," *International Journal of Antennas and Propagation*, vol. 2008, Article ID 642572, 10 pages, 2008. doi:10.1155/2008/642572

[20] S. I. Al-Mously and M. M. Abousetta, "A study of the hand-hold impact on the EM interaction of a cellular handset and a human head," *International Journal of Electronics, Circuits, and Systems* (IJECS), vol. 2, no. 2, pp. 91-95, Spring 2008.

[21] N. Chavannes, R. Tay, N. Nikoloski, and N. Kuster, "Suitability of FDTD-based TCAD tools for RF design of mobile phones," *IEEE Antennas & Propagation Magazine*, vol. 45, no. 6, pp. 52-66, 2003.

[22] M. Martinez-Burdalo, A. Martin, M. Anguiano and R. Villar, "Comparison of FDTD-calculated specific absorption rate in adults and children when using a mobile phone at 900 and 1800 MHz," *Physics in Medicine and Biology*, vol. 49, pp. 345-354, 2004.

[23] *Recommended Practice for Determining the Peak Spatial-Average Specific Absorption Rate (SAR) in the Human Head from Wireless Communications Devices - Measurement Techniques*, IEEE Standard-1528, December 2003.

[24] *Procedure to Measure the Specific Absorption Rate (SAR) in the Frequency Range of 300 MHz to 3 GHz - Part 1: Hand-Held Mobile Wireless communication Devices*, International Electrotechnical Commission, committee draft for vote, IEC 62209.

[25] *Recommended Practice for Determining the Peak Spatial-Average Specific Absorption Rate (SAR) Associated with the Use of Wireless Handsets - Computational Techniques*, draft standard, IEEE-1529.

[26] B. B. Beard and W. Kainz, "Review and standardization of cell phone exposure calculations using the SAM phantom and anatomically correct head models," *Biomedical Engineering Online* 2004, 3:34, 13 October 2004, doi:10.1186/14750925X-3-34.

[27] N. Chavannes, P. Futter, R. Tay, K. Pokovic and N. Kuster, "Reliable prediction of MTE performance under real usage conditions using FDTD," in *Proc.* ICECOM '05, DUBROVINK, October 12-14, 2005.

[28] *SEMCAD-X Reference Manual*, Simulation Platform for Electromagnetic Compatibility, Antenna Design and Dosimetry, SPEAG - Schmid & Partner Engineering AG (see http://www.semcad.com).

[29] K. S. Yee, "Numerical Solution of Initial Boundary Value Problems Involving Maxwell's Equations in Isotropic Media," *IEEE Transaction on Antennas and Propagation*, vol. 14, no.3, pp.302-307, 1966.

[30] *IEEE Standard for Safety Levels with Respect to Human Exposure to Radio Frequency Electromagnetic Fields, 3 kHz to 300 GHz, Amendment 2: Specific Absorption Rate (SAR) Limits for the Pinna*, IEEE Standard C95.1b-2004, December 2004.

[31] M. Burkhardt, "Contributions toward Uncertaint Assessments and Error Minimization of FDTD Simulations Involving Complex Dielectric Bodies," Ph.D. Dissertation, Diss. ETH Nr.13176, Zurich, 1999.

[32] Dielectric Properties of Body Tissue in the frequency range 10 Hz – 100 GHz Italian National Research Council, Institute for Applied Physics, Florence, Italy [online]. Available: http://niremf.ifac.cnr.it/tissprop/

[33] L. Kuo, Y. Kan and H. Chuang, "Analysis of A 900/1800-MHz Dual-Band Gap Loop Antenna on A Handset With Proximate Head and Hand Model," *Journal of Electromagnetic Waves and Applications*, vol. 21, no. 1, 107–122, 2007.